Pergamon

0020–7683(94)E0045–W

STATIC ANALYSIS OF STRUCTURES BY THE QUADRATURE ELEMENT METHOD (QEM)

ALFRED G. STRIZ, WEILONG CHEN and CHARLES W. BERT

School of Aerospace and Mechanical Engineering,
The University of Oklahoma, 856 Asp Avenue, Room 212, Norman, OK 73019, U.S.A.

Abstract—The differential quadrature method (DQM) is an alternative discrete approach to solving directly the governing equations of engineering and mathematical physics. Since the DQM does not require the derivation of the weak forms of the governing equations like the FEM, it can greatly reduce formulation efforts in higher order approximation.

The DQM has been applied in the past to the analyses of various single structural components such as bars, beams, membranes and plates. All of the component analyses yielded good to excellent results. However, previous studies were limited to simple geometries and simple boundary conditions due to the limitation of using global basis functions. In the present study, a domain decomposition technique for the DQM is proposed to analyse truss and frame structures where the whole structural domain is represented by a collection of simple element subdomains connected together at specific nodal points. This method is named the quadrature element method (QEM).

1. INTRODUCTION

Any high accuracy solutions obtained by the standard finite difference method (FDM) or the finite element method (FEM) usually have to be computed based on a large number of discretized points in the computational domain. Consequently, computational efforts are often prohibitive for these numerical techniques. In many cases, the computational effort can be alleviated by using the differential quadrature method (DQM), which was first introduced by Bellman and Casti (1971). Since then, the method has been applied successfully to a variety of problems in structural mechanics [e.g. Bert *et al.* (1988); Jang *et al.* (1989); Sherbourne and Pandey (1991)]. However, there is a certain lack of flexibility when applying this method to real life structural analysis: mapping the physical domain onto the computational domain inflicts a larger loss of efficiency and simplicity on the DQM than on a low order FEM; additionally, difficulties arise from using continuous basis functions to model, e.g. discontinuous loads. For elliptic equations, the above restrictions can be alleviated by the present technique which splits the domain into several subdomains. Since the QEM derives from the strong form of the governing equation, enforcement of the continuity of the function and of its derivative(s) along each internal boundary created by the domain decomposition is required.

Integrating compatibility conditions and techniques to transform the local element weighting coefficients to global element weighting coefficients and then combining the weighting coefficient matrices of all elements, one can construct a global weighting coefficient matrix for the whole structure. By following this systematic procedure, the QEM can be applied to the analysis of structural problems in much the same way as other discretization methods, i.e. the FEM or FDM, but using higher order basis functions than those techniques for better accuracy.

2. GENERAL COMPARISONS OF DQM AND FEM

In this section, three problems were solved by the DQM and the FEM for a direct comparison of the accuracy of the underlying methods. For a second-order system, consider the following ODE:

SAS31:20-E

$$\frac{\mathrm{d}^2 u}{\mathrm{d}x^2} + u + x = 0 \quad 0 \leqslant x \leqslant 1, \tag{1}$$

subject to the boundary conditions $u(0) = u(1) = 0$. The numerical results are plotted in Fig. 1.

For higher order systems, a linearly tapered cantilever beam subject to a concentrated load at one end (fourth-order, Fig. 2) and a curved beam (sixth-order, Fig. 3) were modeled by DQM and FEM. The numerical results are presented in Table 1 and Fig. 3, respectively. For the curved beam example, only half of the circular arch was used for the analysis. More detailed FEM results for tapered beams and DQM modeling schemes for curved members are available in Yang (1986) and Kang *et al.* (1994), respectively. From these three problems, one can see that the accuracy shown by the DQM allows one to obtain solutions with very small errors for second-order systems, or alternatively, to obtain engineering accuracy solutions on coarse meshes for higher order systems.

Generally, the DQM can be viewed as one of a specific class of collocation methods (Bert *et al.*, 1993), which uses the techniques of weighted residuals. That is, the solution of a differential equation is approximated by a linear combination of a set of basis functions. To determine the constants for the approximating solution, the inner product of the residual ε and of a set of weighting functions w_i is forced to be zero:

$$(\varepsilon, w_i) = 0. \tag{2}$$

Instead of locally continuous basis functions like those used, e.g. in the Galerkin method, the DQM uses Dirac delta functions as weighting functions. This results in two advantages. First, because of the use of a collocation approach, one does not need to carry out an integration as shown in eqn (2). Also, one finds the DQ equations easy to formulate, especially in high order approximations which may be cumbersome, e.g. for the Galerkin
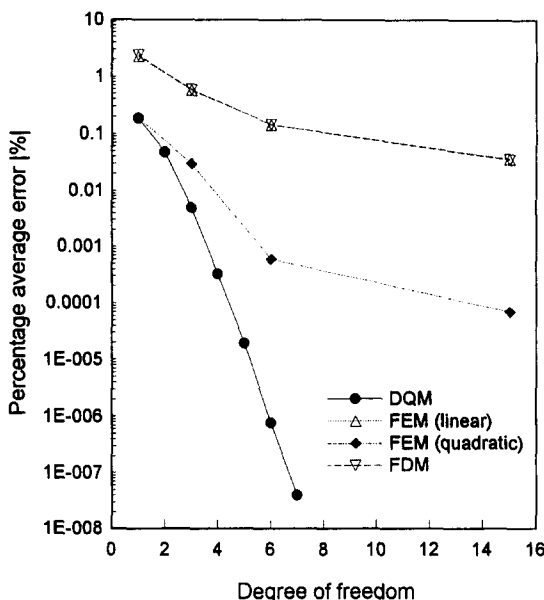

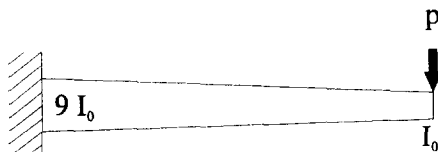Fig. 1. Comparison of numerical results for a second-order equation.

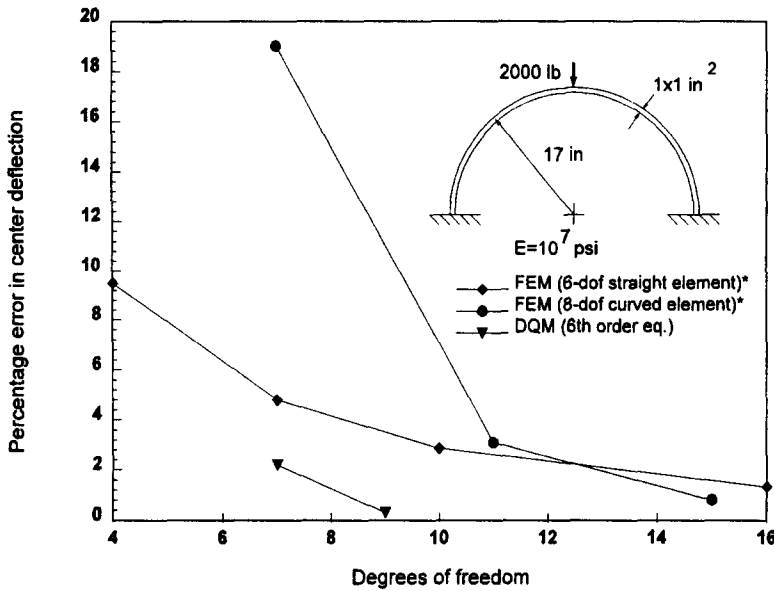Fig. 2. Linearly tapered cantilever beam

Fig. 3. Comparison of numerical results for a circular curved beam problem.

method. Second, for some nonself-adjoint operator equations, for which a weak form formulation would be dificult to obtain, the DQ scheme is still straightforward [e.g. Striz *et al.* (1988)]. Due to these merits, the DQM has proven to be an efficient discretization scheme in many linear and even nonlinear problems [e.g. Bert *et al.* (1989); Wang *et al.* (1993)].

Now, to focus on the development of the QEM, several multi-element structural examples will be illustrated in the following study. The reason behind the selection of these simple structures is that the basis functions used here by the FEM are already complete so as to allow for converged results which will be convenient for direct comparison with the QEM results.

3. APPLICATIONS OF QEM STRUCTURAL ELEMENTS

One can approximate the deformations of bar elements under axial loading and the deflections of beam elements under external forces or moments by polynomial types of solutions. Discontinuities of force or moment may arise from the application of external loads. Therefore, one can apply the QEM and select any geometric, material, force or moment discontinuity point as an interfacing nodal point. The detailed procedures are stated below.

3.1. Truss structures made from bar elements

For a second-order equation model, such as a slender bar with orientation along the

Table 1. Comparisons between DQM and FEM for linearly tapered cantilever beam model

DOF (element)	FEM (uniform elements)		DOF (element)	FEM (tapered elements)		DOF (element)	DQM (tapered element)	
	$\Delta\delta$ $|\%|$	$\Delta\theta$ $|\%|$		$\Delta\delta$ $|\%|$	$\Delta\theta$ $|\%|$		$\Delta\delta$ $|\%|$	$\Delta\theta$ $|\%|$
2 (1)	30.3	10.3	2 (1)	0.62	2.82	3 (1)	0.16	0.74
4 (2)	8.58	5.04	4 (2)	0.17	0.77	4 (1)	0.04	0.19
32 (16)	0.14	0.17	6 (3)	0.06	0.29	5 (1)	0.01	0.05

$\Delta\delta$: error in tip deflection; $\Delta\theta$: error in tip rotation.

x-axis as shown in Fig. 4, the governing equation can be written as

$$\frac{d}{dx}\left(EA\frac{du}{dx}\right) = 0. \tag{3}$$

For a linearly elastic, prismatic bar, the governing equation and the equation of equilibrium become

$$EA\frac{d^2u}{dx^2} = 0; \quad EA\frac{du}{dx} = p. \tag{4}$$

The bar element is discretized by three nodal points as also shown in Fig. 4. Only axial forces are applied at the end points of the bar. Hence, eqns (4) as applied to the nodal points can be expressed as:

$$\text{at point 1}: \frac{du}{dx} = -\frac{p}{EA}; \quad \text{at point 2}: \frac{d^2u}{dx^2} = 0; \quad \text{at point 3}: \frac{du}{dx} = \frac{p}{EA}. \tag{5}$$

Normalizing the variables

$$X \equiv \frac{x}{L}; \quad U \equiv \frac{u}{\alpha}, \tag{6}$$

where α is a reference length, one can rewrite eqn (5) as

$$\frac{dU}{dX} = -\frac{pL}{AE\alpha}; \quad \frac{d^2U}{dX^2} = 0; \quad \frac{dU}{dX} = \frac{pL}{AE\alpha}. \tag{7}$$

Applying DQM to eqn (7) yields

$$\sum_{j=1}^{3} A_{1j}U_j = -P_1; \quad \sum_{j=1}^{3} B_{2j}U_j = 0; \quad \sum_{j=1}^{3} A_{3j}U_j = P_3, \tag{8}$$

where P_i are the non-dimensionalized axial forces. Therefore, in matrix form, one can write

$$[\bar{K}]\{\bar{q}\} = \{\bar{F}\}, \tag{9}$$

where

$$[\bar{K}] = \begin{bmatrix} A_{11} & A_{12} & A_{13} \\ B_{21} & B_{22} & B_{23} \\ A_{31} & A_{32} & A_{33} \end{bmatrix}; \quad \{\bar{q}\} = \begin{Bmatrix} \bar{U}_1 \\ \bar{U}_2 \\ \bar{U}_3 \end{Bmatrix}; \quad \{\bar{F}\} = \begin{Bmatrix} -\bar{P}_1 \\ 0 \\ \bar{P}_2 \end{Bmatrix}$$

are the weighting coefficient matrix, non-dimensionalized displacement vector, and non-dimensionalized force vector, respectively. An overbar represents the local element coordinate system.

Next, to allow for arbitrary orientation of the QEM bar element, a transformation matrix $[T]$ with $\lambda = \cos\theta$ and $\mu = \sin\theta$ is introduced;

$$[T] = \begin{bmatrix} \lambda & \mu & 0 & 0 & 0 \\ -\mu & \lambda & 0 & 0 & 0 \\ 0 & 0 & 1 & 0 & 0 \\ 0 & 0 & 0 & \lambda & \mu \\ 0 & 0 & 0 & -\mu & \lambda \end{bmatrix}. \tag{10}$$

A QEM bar element has three nodal points in the local coordinate system. If one wants to transform these three nodal points to the global coordinate system, that is, decompose the displacement vector into x–y components, one needs a six by six transformation matrix. However, the governing equation for the second point, $d^2u/dx^2 = 0$, implies that the displacement of the point is linearly dependent on the first and the third nodal point. Therefore, to avoid a singular weighting coefficient matrix, this nodal point is not transformed. The transformation of the displacements can then be expressed as

$$\lfloor \bar{U}_1 \ \ 0 \ \ \bar{U}_2 \ \ \bar{U}_3 \ \ 0 \rfloor^T = [T] \lfloor U_1 \ \ V_1 \ \ \bar{U}_2 \ \ U_3 \ \ V_3 \rfloor^T. \tag{11}$$

The transformation matrix $[T]$ is valid for any orientation angle, resulting in coordinate force and coordinate displacement transformations, respectively, as

$$[T]\{F\} = \{\bar{F}\}; \quad [T]\{q\} = \{\bar{q}\}. \tag{12}$$

In terms of eqns (9) and (12),

$$[\bar{K}][T]\{q\} = [T]\{F\} \tag{13}$$

and the global coordinate QEM equation system for a bar element become

$$[K]\{q\} = \{F\}, \tag{14}$$

where

$$[K] \equiv [T]^{-1}[\bar{K}][T].$$

Assembling a global weighting coefficient matrix from all bar element weighting coefficient matrices and solving the combined system matrix, one can get results that match those from the FEM very well for truss problems.

Numerical example 1: *ten-bar truss*. A ten-bar truss was pinned at nodes 1 and 2, and was subjected to a 5000 lb downward load at node 6, as shown in Fig. 5. Let $E = 10^7$ lb/in^2, $L = 10$ in, and $A = 1$ in^2. The numerical results from the QEM were calculated at nodes 5 and 6 and were found to be identical to those from the FEM.
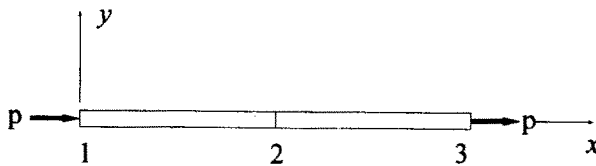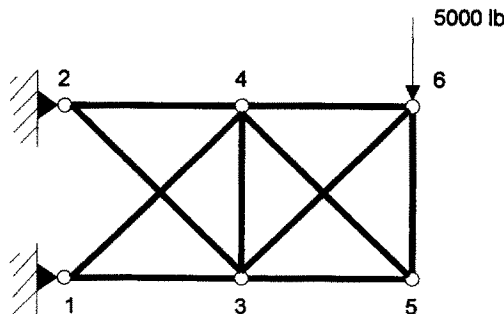

Fig. 4. QEM single bar element.

Fig. 5. Ten-bar truss structure.

3.2. *Beam structures*

For the case of a Bernoulli–Euler beam, the governing equation and the equations of equilibrium for small deformation can be expressed as

$$EI\frac{d^4v}{dx^4} = q(x); \quad EI\frac{d^3v}{dx^3} = f_y; \quad EI\frac{d^2v}{dx^2} = m, \tag{15}$$

where v is the transverse displacement function in the y-direction; E and I denote the modulus of elasticity and the principal moment of inertia about the z-axis, respectively; f_y is the transverse shear force and m is the bending moment.

If only a constant distributed load is considered in a subdomain, a five node DQ model is enough to determine convergent numerical results: two nodes apart a small distance δ at each end of the beam and one node at the middle of the beam. As shown in Fig. 6, these five points are labeled 1–5. Shear forces and moments are applied only at the ends of the beam element, since moment and shear force functions change continuously in the domain between end points 1 and 5. For a small δ, one can assume the approximate relationships

$$m_1 \cong m_2 \quad m_4 \cong m_5; \quad f_{y1} \cong f_{y2} \quad f_{y4} \cong f_{y5}. \tag{16}$$

For a fourth-order equation multidomain problem, the nodal point arrangement is shown in Fig. 7. The domain of element 1 is between nodes 1 and 5, while the domain of element 2 is between 4 and 8. The nodes labeled 4 and 5 are the discretized points common to these two elements, i.e. these two elements have an overlap of two nodal points. Therefore, the slope compatibility condition can be ensured by applying the following constraint:

$$\left.\frac{dy}{dx}\right|_{e2} = \frac{v_5 - v_4}{\delta} = \left.\frac{dv}{dx}\right|_{e1}. \tag{17}$$

Thus, both displacements and rotations satisfy the compatibility conditions automatically in this arrangement.

Applying eqns (15) and (16) to a single beam element as shown in Fig. 6, the DQ five point discretized model can be written as

$$\sum_{j=1}^{5} C_{1j} V_j = F_{y1}; \quad \sum_{j=1}^{5} B_{2j} V_j = M_2; \quad \sum_{j=1}^{5} D_{3j} V_j = Q_3; \quad \sum_{j=1}^{5} C_{4j} V_j = F_{y4}; \quad \sum_{j=1}^{5} B_{5j} V_j = M_5, \tag{18}$$

where $V = v/\alpha$ is the normalized y-deflection v, α is a reference length and $F_y = f_y L^3/EI$,
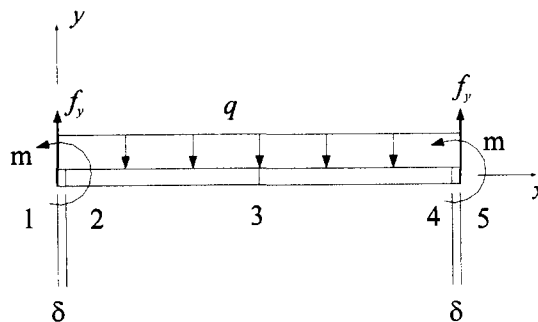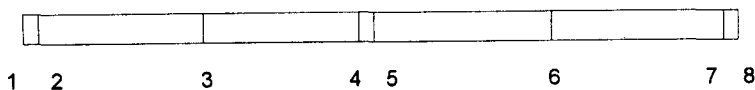

Fig. 6. QEM single beam element.

Fig. 7. Grid spacing for a two-element beam.

$M = mL^2/EI$, and $Q = qL^4/EI$ are the non-dimensionalized shear force, moment and constant distributed load, respectively. Combining two eqns (18) with eqn (17), the following characteristic matrix can be derived for the domain decomposition technique:

$$
\begin{bmatrix}
C_{11}^1 & C_{12}^1 & C_{13}^1 & C_{14}^1 & C_{15}^1 & 0 & 0 & 0 \\
B_{21}^1 & B_{22}^1 & B_{23}^1 & B_{24}^1 & B_{25}^1 & 0 & 0 & 0 \\
D_{31}^1 & D_{32}^1 & D_{33}^1 & D_{34}^1 & D_{35}^1 & 0 & 0 & 0 \\
C_{41}^1 & C_{42}^1 & C_{43}^1 & C_{44}^1+C_{11}^2 & C_{45}^1+C_{12}^2 & C_{13}^2 & C_{14}^2 & C_{15}^2 \\
B_{51}^1 & B_{52}^1 & B_{53}^1 & B_{54}^1+B_{21}^2 & B_{55}^1+B_{22}^2 & B_{23}^2 & B_{24}^2 & B_{25}^2 \\
0 & 0 & 0 & D_{31}^2 & D_{32}^2 & D_{33}^2 & D_{34}^2 & D_{35}^2 \\
0 & 0 & 0 & C_{41}^2 & C_{42}^2 & C_{43}^2 & C_{44}^2 & C_{45}^2 \\
0 & 0 & 0 & B_{51}^2 & B_{52}^2 & B_{53}^2 & B_{54}^2 & B_{55}^2
\end{bmatrix}
\begin{Bmatrix} V_1 \\ V_2 \\ V_3 \\ V_4 \\ V_5 \\ V_6 \\ V_7 \\ V_8 \end{Bmatrix}
=
\begin{Bmatrix} F_{y1} \\ M_2 \\ Q_3 \\ F_{y4} \\ M_5 \\ Q_6 \\ F_{y7} \\ M_8 \end{Bmatrix},
$$

$$(19)$$

where $(\ )^i$ represents the weighting coefficient of the ith element and V_k represents the non-dimensionalized deflection at the kth nodal point for the grid spacing arrangement shown in Fig. 7. After the deflections are found from eqn (19), the rotation at each internal point in the QEM element can be calculated from eqn (20):

$$\{\theta\} = \{\bar{\theta}\} = [\bar{A}]\{\bar{q}\}. \tag{20}$$

Numerical example 2: *cantilever and simply supported beams.* Numerical results derived using eqns (19) and (20) for a two-element cantilever beam model with various loading conditions are shown in Table 2.

Increasing the number of internal discretized points, one can apply this method easily to non-smooth loading conditions for which the DQM may not be suitable. A comparison of results for a simply supported beam under a triangular load is listed in Table 3.

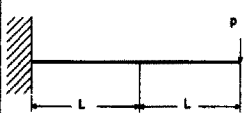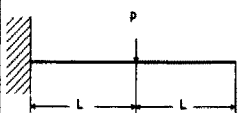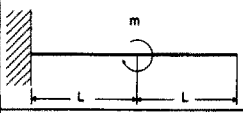Table 2. Two-element QEM cantilever beam under various loads
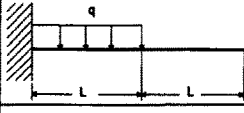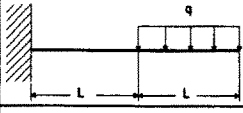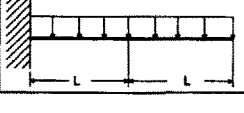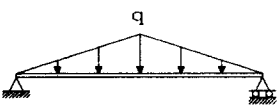
Loading Conditions	Error |%|	Loading Conditions	Error |%|
	$\Delta v = 0.016$ $\Delta \theta = 0.016$		$\Delta v = 0.016$ $\Delta \theta = 0.005$
	$\Delta v = 0.016$ $\Delta \theta = 0.012$		$\Delta v = 0.016$ $\Delta \theta = 0.016$
	$\Delta v = 0.016$ $\Delta \theta = 0.007$		$\Delta v = 0.016$ $\Delta \theta = 0.016$
	$\Delta v = 0.016$ $\Delta \theta = 0.016$	Δv : Error in tip deflection $\Delta \theta$: Error in tip rotation $\delta = 0.00001$	

Table 3. Comparison of DQM and QEM under non-smooth distributed load

Loading Conditions	Solutions	DQM	QEM
	Number of elements	1	2
	D. O. F.	9	10
	Error in center |%|	8.4	0.016

3.3. *Frame structures made from beam elements*

Recall that one can relate local displacements $\bar{u}$, $\bar{v}$ to global displacements u, v of a beam element arbitrarily oriented in the plane by using

$$\begin{Bmatrix} \bar{u} \\ \bar{v} \end{Bmatrix} = \begin{bmatrix} \cos\theta & \sin\theta \\ -\sin\theta & \cos\theta \end{bmatrix} \begin{Bmatrix} u \\ v \end{Bmatrix}. \tag{21}$$

Then, we can consider a transformation

$$[T] \lfloor u_1 \ v_1 \ \theta_2 \ u_3 \ v_3 \ u_4 \ v_5 \ \theta_5 \rfloor^T = \lfloor \bar{u}_1 \ \bar{v}_1 \ \theta_2 \ \bar{u}_3 \ \bar{v}_3 \ \bar{u}_4 \ \bar{v}_5 \ \theta_5 \rfloor^T. \tag{22}$$

For a single five point quadrature beam element as in the previous section, a transformation matrix $[T]$ can be defined by

$$[T] = \begin{bmatrix} \lambda & \mu & 0 & 0 & 0 & 0 & 0 & 0 \\ -\mu & \lambda & 0 & 0 & 0 & 0 & 0 & 0 \\ 0 & 0 & 1 & 0 & 0 & 0 & 0 & 0 \\ 0 & 0 & 0 & \lambda & \mu & 0 & 0 & 0 \\ 0 & 0 & 0 & -\mu & \lambda & 0 & 0 & 0 \\ 0 & 0 & 0 & 0 & 0 & \lambda & \mu & 0 \\ 0 & 0 & 0 & 0 & 0 & -\mu & \lambda & 0 \\ 0 & 0 & 0 & 0 & 0 & 0 & 0 & 1 \end{bmatrix}, \tag{23}$$

with $\lambda = \cos\theta$ and $\mu = \sin\theta$ to arbitrarily orient the beam element in the plane. Similar to the transformation techniques used in the bar, one can then calculate the global coordinate system equations as

$$[K]\{q\} = \{F\}, \tag{24}$$

where

$$[K] = [T]^T[\bar{K}][T] \tag{25}$$

is the global weighting coefficient matrix. Moreover, if one combines the weighting coefficients of the axial force bar element in the *x*-direction from eqn (9) and the weighting coefficients of the cantilever beam element in the *y*-direction from eqn (18), the local weighting coefficient matrix for the *i*th frame element can be written as

$$[\bar{K}] = \begin{bmatrix} A'^{i}_{11} & 0 & 0 & A'^{i}_{12} & 0 & A'^{i}_{13} & 0 & 0 \\ 0 & C^{i}_{11} & C^{i}_{12} & 0 & C^{i}_{13} & 0 & C^{i}_{14} & C^{i}_{15} \\ 0 & B^{i}_{21} & B^{i}_{22} & 0 & B^{i}_{23} & 0 & B^{i}_{24} & B^{i}_{25} \\ A'^{i}_{21} & 0 & 0 & A'^{i}_{22} & 0 & A'^{i}_{23} & 0 & 0 \\ 0 & D^{i}_{31} & D^{i}_{32} & 0 & D^{i}_{33} & 0 & D^{i}_{34} & D^{i}_{35} \\ A'^{i}_{31} & 0 & 0 & A'^{i}_{32} & 0 & A'^{i}_{33} & 0 & 0 \\ 0 & C^{i}_{41} & C^{i}_{42} & 0 & C^{i}_{43} & 0 & C^{i}_{44} & C^{i}_{45} \\ 0 & B^{i}_{51} & B^{i}_{52} & 0 & B^{i}_{53} & 0 & B^{i}_{54} & B^{i}_{55} \end{bmatrix} . \tag{26}$$

In eqns (26), $(\ )^{i}$ means the ith element, $(\ )'$ means the weighting coefficients for the axial effect. Again, the rotations of the nodal points can be calculated from $\{\theta\} = \{\bar{\theta}\} = [\bar{A}]\{\bar{q}\}$.

Compatibility conditions and global formulation. When connecting two arbitrarily oriented beam elements, only one nodal point is used to connect the two elements. The discretized nodal points near the junction are shown in Fig. 8. Node a is the point that belongs to both elements. Therefore, displacement compatability is satisfied automatically. Since the distances between a–b and a–c are very small, one can assume that these points keep the same orientation after deformation, that is, the rotation of segment ab is the same as the rotation of segment ac. The first-, second- and third-order compatibility conditions can be derived by applying the constraints:

$$\left. \frac{d\bar{v}}{dx} \right|_{e1} - \left. \frac{d\bar{v}}{dx} \right|_{e2} = 0; \quad m^{a}_{e1} + m^{c}_{e2} + m_{ext} = 0; \quad f^{b}_{e1} + f^{a}_{e2} + f_{ext} = 0 \tag{27}$$

at points a, b and c, respectively. Assembling the weighting coefficients as shown in eqn (19), one can express the QEM model for a frame structure in the form

$$[K^{*}]\{q^{*}\} = \{F^{*}\}. \tag{28}$$

By inverting $[K^{*}]$, one can obtain the deflection vector as

$$\{q^{*}\} = [K^{*}]^{-1}\{F^{*}\}, \tag{29}$$

where $[K^{*}]$ represents the combined weighting coefficient matrix for the whole structure.

From the previous section, it is clear that, when δ is small enough, the deflections of the two neighboring points are essentially the same, i.e. in Fig. 6,

$$u_{1} \cong u_{2}, \quad v_{1} \cong v_{2}, \quad u_{4} \cong u_{5}, \quad v_{4} \cong v_{5}. \tag{30}$$

For convenience and to avoid confusion in the following modeling of frames, nodal points
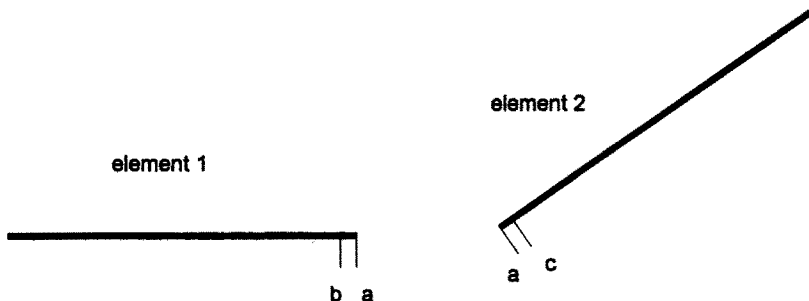
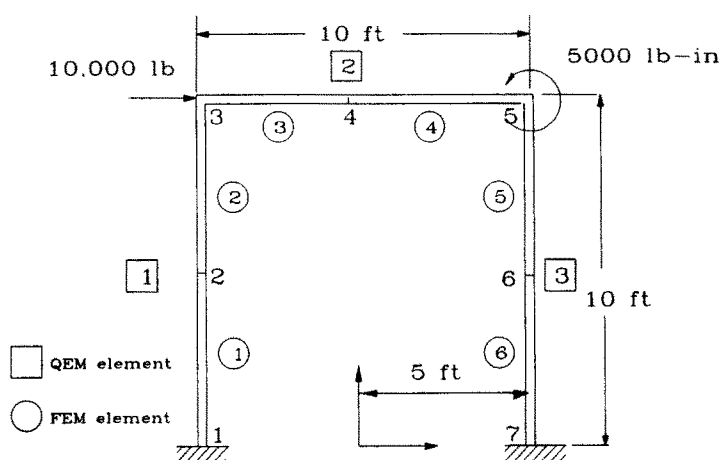Fig. 8. Nodal point arrangement at the element interface.

Fig. 9. Portal frame structure.

separated by δ will, therefore, be denoted by a single node number. Thus, for an arbitrarily oriented frame element, only the 1, 3 and 5 nodal points of each element are labeled by specific numbers in the following three simple frame structure examples.

Numerical example 3 : *simple frame structure* (Logan, 1986). Consider the plane frame problem of a portal frame (Fig. 9). The frame is fixed at nodes 1 and 7 and subjected to a positive horizontal force of 10,000 lb applied at node 3 and to a positive moment of 5000 lb·in at node 5. Let $E = 30 \times 10^6$ psi and $A = 10$ in^2 for all elements, and let $I = 200$ in^4 for QEM elements 1 and 3 and $I = 100$ in^4 for QEM element 2. The numerical results from the QEM are listed in Table 4 together with FEM results, showing excellent comparison.

Numerical example 4 : *frame subjected to distributed loads* (Logan, 1986). A frame, as shown in Fig. 10, is fixed at nodes 1 and 5 and subjected to a uniformly distributed load of 1000 lb/ft applied downward over the horizontal QEM element. The global coordinate axes have been established at node 1. Let $E = 30 \times 10^6$ psi, $A = 100$ in^2 and $I = 10,000$ in^4 for both elements of the frame. The numerical results obtained by QEM and FEM compare very well as shown in Table 5.

Numerical example 5 : *three-element frame* (Logan, 1986). A frame as shown in Fig. 11 is subjected to a 15-kip horizonal load applied at the mid-length of QEM element 1. Nodes 1, 5 and 7 are fixed. Let $E = 30 \times 10^6$ psi, $I = 800$ in^4 and $A = 8$ in^2 for all elements. The numerical results are listed in Table 6.

Table 4. Numerical results for a portal frame

Disp. or Rot.	FEM $(15 \times 15)^*$ (in, rad)	QEM $(12 \times 12)^*$ (in, rad)
u_3	2.1136×10^{-1}	2.1130×10^{-1}
v_3	1.4813×10^{-3}	1.4813×10^{-3}
θ_3	-1.5206×10^{-3}	-1.5258×10^{-3}
u_4	2.1036×10^{-1}	2.1030×10^{-1}
v_4	-6.0050×10^{-5}	-6.0373×10^{-5}
θ_4	7.1598×10^{-4}	7.1583×10^{-4}
u_5	2.0936×10^{-1}	2.0930×10^{-1}
v_5	-1.4813×10^{-3}	-1.4813×10^{-3}
θ_5	-1.4860×10^{-3}	-1.4857×10^{-3}

* To compare deflections and rotations at every nodal point for this three-element frame, six FEM beam elements were used. Here, the matrix size of the FEM was 15 by 15, while the matrix size of the DQM was 12 by 12, because the rotation of each center nodal point can be calculated in terms of the displacements in the DQM.
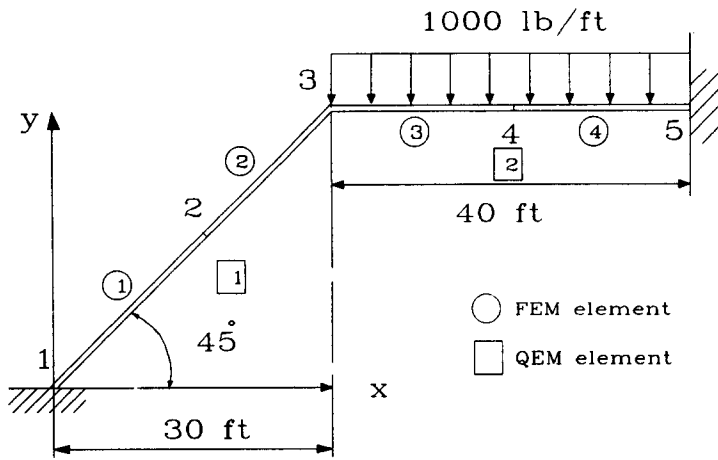
Fig. 10. Frame under distributed load.

Table 5. Numerical results for a frame under distributed load

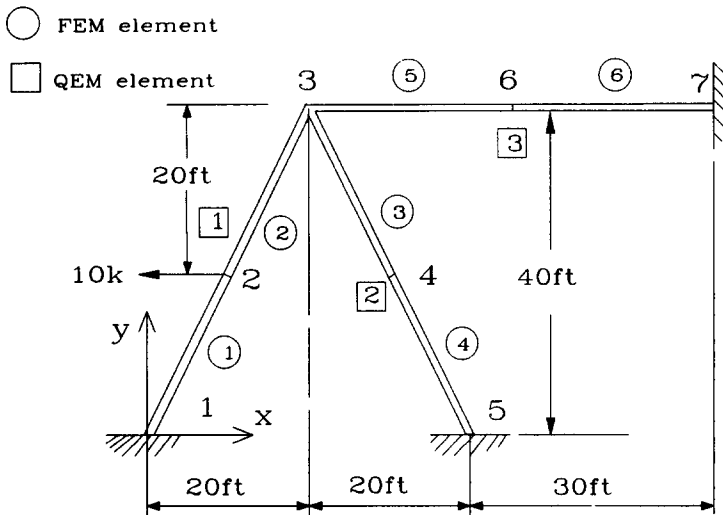| Disp. or Rot.	FEM (9 × 9) (in, rad)	QEM (7 × 7) (in, rad)
u_3	3.2950×10^{-3}	3.2945×10^{-3}
v_3	-9.7422×10^{-3}	-9.7419×10^{-3}
θ_3	-3.2917×10^{-3}	-3.2903×10^{-3}

Fig. 11. Three-element frame structure.

Table 6. Numerical results for three-element frame

Disp. or Rot.	FEM (12 × 12) (in, rad)	QEM (9 × 9) (in, rad)
u_3	1.030×10^{-2}	1.027×10^{-2}
v_3	9.56×10^{-4}	9.59×10^{-4}
θ_3	1.030×10^{-3}	1.030×10^{-3}

In all three examples, the QEM characteristic matrix to be inverted was smaller than the FEM stiffness matrix.

4. CONCLUSIONS AND RECOMMENDATIONS

The previous study demonstrates the applicability of the QEM to the analysis of truss and frame structures under various loading conditions. For second-order equation systems, e.g. the ten-bar truss model, the QEM gives exactly the same results as the FEM since the assumed displacement functions of both methods are complete to ensure converged results. When higher order approximations are needed as in tapered bar or vibration problems, the QEM delivers better results than the lower order FEM schemes for the same number of degrees of freedom due to the high order of the basis functions. For fourth-order equation systems, minor discrepancies to the FEM are observed even though the assumed basis functions are complete for exact solutions. The differences are caused by using the approximating δ to treat multiple boundary conditions, a scheme adopted for the fourth-order DQ solution method. To minimize the adverse effects caused by the δ-type grid arrangements, a matrix condensation technique used by Jang (1987) will alleviate the truncation errors caused by this kind of approximation. Also, various refinements and improvements to the treatment of boundary conditions and to convergence have been proposed recently by Wang and Bert (1993) and Striz et al. (1993). However, even the present QEM is very efficient in achieving engineering accuracy in structural truss and frame analyses, requiring a smaller stiffness matrix to be inverted than the FEM for comparable results. In addition, in frame problems, one can easily apply distributed loads at the discrete nodal points defined by the QEM instead of having to use the equivalent force method as in the FEM.

Overall, the QEM is easily formulated and allows for the efficient solution of structural truss and beam problems. It combines the attractive features of rapid convergence and high accuracy of the DQM with the generality of the FEM element formulation in application to structural analyses. The extension of this method to two-dimensional rectangular and curvilinear elements is presently underway.

REFERENCES

Bellman, R. E. and Casti, J. (1971). Differential quadrature and long-term integration. *J. Math. Anal. Applic.* **34**, 235–238.

Bert, C. W., Jang, S. K. and Striz, A. G. (1988). Two new approximate methods for analysing free vibration of structural components. *AIAA J.* **26**, 612–618.

Bert, C. W., Jang, S. K. and Striz, A. G. (1989). Nonlinear bending analysis of orthotropic rectangular plates by the method of differential quadrature. *Comput. Mech.* **5**, 217–226.

Bert, C. W., Wang, X. and Striz, A. G. (1993). Differential quadrature for static and free vibration analyses of anisotropic plates. *Int. J. Solids Structures* **30**(13), 1737–1744.

Jang, S. K. (1987). Application of differential quadrature to the analysis of structural components. Ph.D. Dissertation, The University of Oklahoma, Norman, OK.

Jang, S. K., Bert, C. W. and Striz, A. G. (1989). Application of differential quadrature to deflection and buckling of structural components. *Int. J. Numer. Meth. Engng* **28**, 561–577.

Kang, K., Bert, C. W. and Striz, A. G. (1994). Differential quadrature method for vibration and buckling analysis of circular arches. Unpublished manuscript.

Logan, D. L. (1986). *A First Course in the Finite Element Method.* PWS Engineering, Boston.

Sherboune, A. N. and Pandey, M. D. (1991). Differential quadrature method in the buckling analysis of beams and composite plates. *Comput. Struct.* **40**, 903–913.

Striz, A. G., Chen, W. L. and Bert, C. W. (1993). Convergence of the DQ method in the analysis of fourth-order equation systems. Unpublished manuscript.

Striz, A. G., Jang, S. K. and Bert, C. W. (1988). Nonlinear bending analysis of thin circular plates by differential quadrature. *Thin-Walled Struct.* **6**, 51–62.

Wang, X. and Bert, C. W. (1993). A new approach in applying differential quadrature to static and free vibrational analyses of beams and plates. *J. Sound Vibr.* **162**(3), 566–572.

Wang, X., Bert, C. W. and Striz, A. G. (1993). Differential quadrature analysis of deflection, buckling and free vibration of beams and rectangular plates. *Comput. Struct.* **48**(3), 473–479.

Yang, T. Y. (1986). *Finite Element Structural Analysis.* Prentice-Hall, Englewood Cliffs, NJ.